

Article

A Precise Simultaneous Sowed Control System for Maize Seed and Fertilizer

Jinxin Liang^{1,2,3} , Feng Pan^{1,3}, Jincheng Chen^{1,3}, Hui Zhang^{1,3} and Chao Ji^{1,3,*}

¹ Mechanical Equipment Research Institute, Xinjiang Academy of Agricultural and Reclamation Science, Shihezi 832000, China

² College of Mechanical and Electrical Engineering, Shihezi University, Shihezi 832003, China

³ Key Laboratory of Northwest Agricultural Equipment, Ministry of Agriculture and Rural Affairs, Shihezi 832003, China

* Correspondence: jicobear@163.com; Tel.: +86-185-0993-6173

Abstract: To improve the utilization rate of maize seed fertilizer, this study aimed to propose a precise co-sowing control system for the real-time control of the relative position of seed fertilizer during the co-sowing operation. According to the operating speed of the machine, the longitudinal distance between the seed feeder and the outer groove wheel, the height of the seed and fertilizer falling, and the relative position of the seed and fertilizer falling into the soil, the calculation method for the seed and fertilizer falling into the soil was obtained, the precise co-seeding model of the seed fertilizer was constructed, the control algorithm of the precise co-seeding of the seed fertilizer was designed, and the hardware system and software system were designed. Based on the hardware structure and working principle of the motor drive seeding and fertilization control system, a functional circuit based on the STM32F103ZET6 single-chip microcomputer (Zhengdianyuanzi (Guangzhou) Technology Co., Ltd., Guangzhou, China) was built. When the system is working, the satellite speed measurement module collects the operating speed of the machine, the encoder feeds back the motor speed in real time, a Hall sensor detects the time interval between fertilizer and seed discharge at the point of discharge, and the PID algorithm is applied to make the speed regulation system regulate the motor speed and position and adjust the speed and position of the seed discharge tray and fertilizer on the outer slot wheel in real time. The relative position of seed and fertilizer in the soil can be controlled accurately in the process of sowing fertilizer. The test results showed that when the feed speed was 2, 3, and 4 km·h⁻¹, and the grain spacing was 20, 25, and 30 cm, respectively, the seed fertilizer alignment was better and met the requirements of precise sowing, improving fertilizer utilization rate.



Citation: Liang, J.; Pan, F.; Chen, J.; Zhang, H.; Ji, C. A Precise Simultaneous Sowed Control System for Maize Seed and Fertilizer. *Agriculture* **2024**, *14*, 192. <https://doi.org/10.3390/agriculture14020192>

Received: 28 December 2023

Revised: 16 January 2024

Accepted: 18 January 2024

Published: 26 January 2024



Copyright: © 2024 by the authors. Licensee MDPI, Basel, Switzerland. This article is an open access article distributed under the terms and conditions of the Creative Commons Attribution (CC BY) license (<https://creativecommons.org/licenses/by/4.0/>).

Keywords: accurate simultaneous sowing; seed fertilizer location; real-time control; motor drive

1. Introduction

Sowing and fertilization are an important part of maize field production. The quality of these operations has an important impact on controlling the cost of agricultural materials, increasing crop yield, and improving planting income. Unreasonable fertilization methods will lead to a low fertilizer utilization rate, resulting in waste of fertilizer, thereby increasing agricultural production costs [1]. At present, production efficiency is mainly improved by maize seed and fertilizer co-sowing technology, which can not only save time and energy but also improve the utilization rate of fertilizer [2]. The fertilization method for maize seed and fertilizer-integrated machines mostly adopts strip fertilization [3,4]. The concentration of fertilizer is convenient for operation and easy to achieve for the purpose of deep application, but the application of fertilizer is easy to overdo [5,6]. Excessive use of chemical fertilizers can pollute the ecological environment, cause soil compaction, and burn seeds easily [7–9]. Hole fertilization is usually located on one side of the sowing position or the rear side of the sowing position. Fertilizer is applied into a reasonable

position according to a certain number of holes. The recommended depth for seed fertilizer is 5 cm, the horizontal distance of seed fertilizer is 3~7 cm, the vertical distance of seed fertilizer is 3~5 cm, and the distance between fertilizer and seed should be more than 5 cm to prevent seed burning [4,10,11]. Hole fertilization is a more centralized method of fertilizer application than strip fertilization [12], and it can achieve the purpose of reducing fertilizer and increasing yield [13–16]. There are still shortcomings in the intelligent degree of sowing and fertilizing machines [17]. The seeding and fertilizing machines mainly rely on a ground wheel to drive the rotation of the seed plate and a groove wheel to realize the seeding and fertilizing operations. In the actual field operation environment, the ground wheel is easily affected by the ground conditions, resulting in problems such as jumping and slipping [18,19], which seriously affect the accuracy of sowing and fertilization. High precision is the development trend for the seeder. The improvement of mechanical properties alone cannot meet the requirements of high precision [20,21]. Using advanced motor control and measurement [22,23] and control technology based on seed and fertilizer sowing technology is a new way to solve the above problems, and it is also an inevitable requirement to improve the intelligence of seeders [20].

In recent years, with the development of industrial technologies such as motor power and intelligent control in China, the research and development on the design of electric drive agricultural machinery equipment has become a research hotspot. Heilongjiang Dewo and Shandong Leiwo have developed the initial models of electric drive precision seeders and carried out popularization and application, but they have not yet integrated the function of precise simultaneous sowing of seeds and fertilizer. Corn planters are developing in the direction of high speed and high precision, and must meet the development requirements of precision agriculture [1,24]. The research on maize burrow fertilization machinery in China is still in the initial stage, with more of the research being conducted by colleges, universities, and research institutes. Liu et al. [25] designed an automatic maize seed hole fertilization device and proposed an automatic seeding method based on a planetary gear train. Under the premise of ensuring that the seed spacing and fertilizer spacing were equal, the phase difference between the seed plate and the fertilizer plate was adjusted in real time to realize the real-time control of the relative position of the seed and fertilizer during the sowing operation. Wang et al. [26] designed an intelligent maize variable hole fertilization control system. The opening and closing of the fertilizer outlet baffle were controlled by a stepper motor to realize the hole fertilization of maize. Wu et al. [27] designed a hole fertilization device that can achieve precise hole seeding and fertilizer control. A rocker mechanism directly controls the opening and closing of a duckbill apparatus, and the opening and closing of the duckbill valve need to operate at a high frequency. Dong et al. [28] designed an intermittent fixed-point hole-type rice-side deep fertilization device. The main structure was a spiral fertilizer discharge component, which realized the side-deep fertilization operation for rice. Liao et al. [29] designed a mechanical hole fertilization device and proposed a deep hole fertilization process for application on the side of rape plants. The fertilizer was deeply applied to the side of the rape root system, and the fertilizer particles were distributed in a hole shape. The fertilizer discharger was divided into holes according to a certain time interval. An intermittent fertilization device designed by Zhang et al. [30] controls the opening and closing of a turnover plate with a single-chip microcomputer, and the fertilizer is discharged into a layered fertilization tube through the intermittent opening and closing of the turnover plate. A fertilizer applicator designed by Zhou et al. [31] uses a groove wheel mechanism with controllable speed to control the amount of fertilizer applied under the soil through a duckbill discharge port. The above scholars have provided new ideas for research on hole fertilization devices, but the structures of their designed devices are more complex, and the performance of the hole insertion mechanisms is greatly affected by soil conditions and operating speed, so it is difficult to put them into practical production and application. There are many mechanical methods to achieve precise fertilization, and most hole fertilization devices have better hole-forming performance. However, there are few studies on intelligent control, and there

is a lack of devices for regulating the position of seeds and fertilizer. The relative position of seed and fertilizer is affected by many factors, such as the forward speed of the machine, the spacing of the seed metering device, and the seed spacing. It is difficult to realize the real-time regulation of the relative position of seed and fertilizer in the seeding process through a single mechanical structure. It is necessary to design a special seed and fertilizer matching system.

As a key part of technological change, the precision operation control system is the core content of related research work. It is necessary to focus on the completion of the cooperative operation function of seed and fertilizer, to control the spatial distribution of seed and fertilizer, achieve the precise alignment of seed and fertilizer into the soil, to improve the sowing quality and fertilizer utilization rate, and realize a reduction in fertilizer and efficiency. Therefore, the main objective of this study was to develop a precise co-seeding control system for corn fertilizer and test its accuracy. However, the specific objectives of this study were (1) to build a co-sowing device for corn fertilizer; (2) to construct a precise co-seeding model and algorithm of maize fertilizer; (3) to adjust the parameters of the motor of the device and test the accuracy of the developed system on this basis.

2. Materials and Methods

2.1. Plant Materials and Field Conditions

According to the nutrients required for the growth cycle of maize, soil fertility, target yield, and local fertilization habits generally determine the amount of fertilizer applied to a single maize plant. The growth cycle of maize in Shihezi City, Xinjiang Uygur Autonomous Region, China, was taken as an example, and polypore urea (Shihezi Jintun Agrochemical Co., Ltd., Shihezi, China) was selected as the fertilization test material. The sowing test material was Xinyu No. 9 hybrid maize seed, which the Crop Research Institute of Xinjiang Academy of Agricultural and Reclamation Science produced. The moisture content was 9.1%, the 8-degree was 98.75%, and the 1000-seed weight was (274.22 ± 2.52) g [32]. Three hundred seeds were randomly measured. The shape was horse-tooth, and the length, width, and height dimensions were (10.04 ± 1.06) mm, (7.45 ± 0.86) mm, and (5.50 ± 1.01) mm [33]. The test site was selected in the soil tank laboratory of Xinchangsheng Agricultural Machinery Company, Shihezi, China. The experimental plot was flat and had no obstacles. The quality of soil preparation meets the requirements of agricultural technology. The length of the test area was more than 50 m, the size of the preparation area at both ends was not less than 10 m, and the width was more than 2 m, which meets the requirements of the experimental project.

2.2. Precise Simultaneous Sowed Control System

The control system hardware architecture integrates multiple essential circuits; notably, it features an STM32 microcontroller core to manage operations, an encoder interface for position feedback, a serial port debugging setup for diagnostics, a hall effect speed sensing mechanism, a dedicated power supply circuit, and a satellite GPS speed measurement receiver, along with any other ancillary components. The HS6602-485 GPS/Beidou dual-mode positioning module (Shandong Huxin Intelligent Technology Co., Ltd., Jinan, China) was selected to obtain the machine's working speed. The working voltage is 5 V, the detection accuracy is $0.1 \text{ m}\cdot\text{s}^{-1}$, the update frequency is 1~10 Hz, and the communication protocol is Modbus. The positioning information is transmitted to the microcomputer through the RS485 standard communication port with a baud rate capability of 115,200 bps. Regarding sensor installation, magnetic beads have been meticulously placed just under each seed hole in the seed plate. Along the rotation path of the outer groove wheel, matching magnetic beads are embedded at corresponding positions within the grooves. Additionally, hall sensors are affixed to the casing of both the seed metering apparatus and the fertilization box housing to facilitate precise tracking. The STM8-P12 and 545-P16 AB phase hall encoders (Bengbu Juhua Network Technology Co., Ltd., Benbu, China)

are used to detect the speed of the fertilizer and seeding motors, respectively. To ensure precise monitoring of the motor's rotation, the encoder plate was professionally welded onto the motor's tail-end electrode and solidly anchored. The magnetic ring component is attached to the motor's tail shaft and revolves in tandem with it. A hall effect sensor is integrated within the system which adeptly transforms the mechanical angular velocity of the motor's rotation into a digital signal composed of alternating high and low levels. These signals are then conveyed to the microcontroller by way of the A/B phase channels. This particular module runs on a power supply voltage of 3 V. For voltage regulation, we deploy an SD-350C-12 power module (Taizhou Mingwei Automation Co., Ltd., Wenzhou, China), which efficiently reduces 48 V to a steady 12 V, catering to the power needs of the entire setup. We selected the NJK-5001A (CHE8-10PA-H710)-type hall sensor (Zhejiang Huchuang Electric Co., Ltd., Wenzhou, China), with a sensor rated current of 300 mA, rated operating voltage of 5~30 V, effective detection distance of 10 mm, rapid induction, accurate detection, output mode PNP-NO, response time below 2 ms, and thread diameter model M 8. The hardware components of the control system are illustrated in Figure 1.

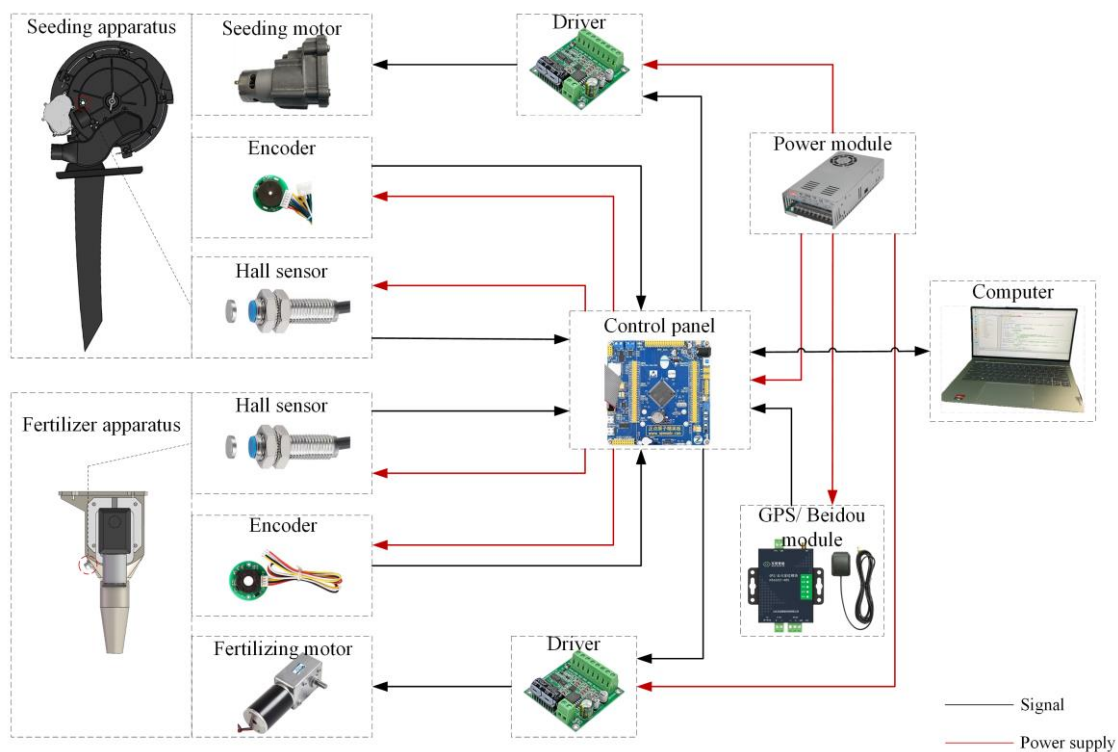


Figure 1. Control system structure diagram.

We chose the air suction precision metering device (Precision Planting Company, Normal, America) for its accuracy and efficiency. The diameter of the seed hole is 4.5 mm, and the number of seed holes is 9. The outer groove wheel fertilizer distributor was selected. The outer groove wheel has 3 grooves, the span of a single groove is 30°, and the diameter of the outer groove wheel is 70 mm. The seeding DC motor adopts the NC3SFN-6035-CVC carbon brush variable resistance brush DC motor (Transmotec Company, Stockholm, Sweden). The working voltage for this seeding motor is DC 12 V, the current is 5.6 A, the rated speed is 10,700 r·min⁻¹, and the rated torque is 0.4468 N·m. The motor reducer adopts the three-stage deceleration gear mechanism developed by Heilongjiang Devo, and its deceleration ratio is 82.8125, which can provide enough torque to drive the seeding plate for the seeding DC motor. The fertilization DC motor uses the A58-555-1280 encoder DC motor (Shenzhen Xinyongtai Hardware Electronics Co., Ltd., Shenzhen, China). The working voltage is 12 V, the current is 6.3 A, and the rated speed is 3100 r·min⁻¹. The motor reducer has a 16:1 reduction ratio and a torque of 1.0 N·m. The rated torque is the

meshing transmission of the power output gear of the DC motor reducer and the outer gear of the seeding plate. We chose an Aisikong type AQMH3615NS-B DC motor (Chengdu Aikong electronic technology company, Chengdu, China) driver, suitable for the selected seed DC motor and fertilizer DC motor; the input voltage is DC 9~36 V, which can drive the rated voltage of a 12 V DC motor, the maximum load current is 12 A without heat dissipation, and it has three-wire control speed regulation, positive and negative rotation, and braking. The PWM effective range is 0.1~100.0%, and it can provide a 5 V power supply for single-chip microcomputer and interface with ESD protection.

The control flow of the automatic seed fertilization system is illustrated in Figure 2. Upon powering on, the system operates based on user-defined parameters, including seed spacing, the distance and height between the seed metering device and fertilizer extractor, and the number of holes on the seed metering plate.

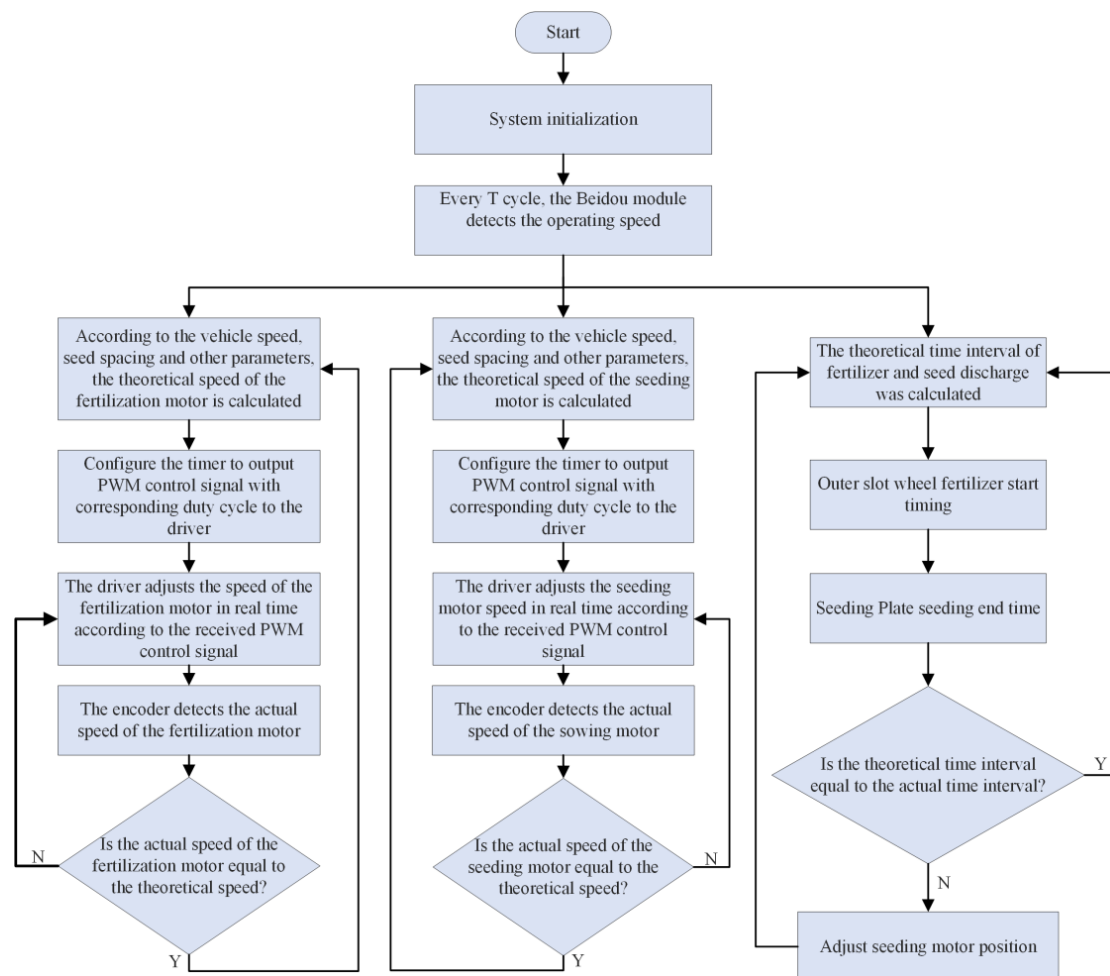


Figure 2. Flow chart of fertilizer alignment control system.

The GPS/Beidou module from Shandong Huxin Intelligent Technology Co., Ltd. in Jinan, China, detects the machine's forward speed. The STM32 single-chip microcomputer from Zhengdianyuanzi (Guangzhou) Technology Co., Ltd. in Guangzhou, China, calculates the theoretical speed of the drive motor in real time. The motor speed sensor detects the speed of the seeding and fertilizer motor in real time. The hall sensor detects the time the fertilizer and seed are discharged. It starts when the fertilizer discharge device detects fertilizer information and stops when the seed discharge signal is detected. The position relation of the seed fertilizer determines the seed discharge time of the seed discharge device. The relative position of the seed and the hole fertilizer is obtained by comparing the theoretical and actual values. The fuzzy PID position ring adjusts the relative position

of the seed and fertilizer until the surface seed corresponds to the fertilizer position. It does not work when the seed corresponds to the fertilizer position in the hole, which is when the time of the seeding plate corresponds to the theoretical time. When the seed does not correspond to the hole fertilizer, the fuzzy PID position ring works, and the seed discharge motor accelerates or decelerates to adjust the relative position of the seed and fertilizer.

2.3. Structure

The precise co-sowing device for maize seed and fertilizer consists of a seeding unit, fertilization unit, control unit, and link mechanism. The sowing unit includes an air suction seed metering device and seed guide tube, while the fertilization unit is mainly composed of a fertilizer apparatus and fertilizer guide tube. The control unit is made up of an STM32 single-chip microcomputer, velocity measurement module, DC motor, and detection module. The structure of the device is shown in Figure 3. The working principle is as follows. The fertilization unit is installed in front of the sowing unit, with a certain transverse distance between them to allow for deep hole fertilization on the side of the maize seed. During operation, the outer slot wheel fertilizer dispenser takes pelleted fertilizer from the fluted roller fertilizer apparatus and applies it into the fertilizer ditch through the fertilizer guide pipe. In the seeding unit, the air suction seed dispenser ensures precise seed discharge. Sensors are installed in both the fertilizer dispenser and seed dispenser, with magnetic beads placed directly below the seed hole of the seed dispenser and hall sensors located on the back of the seed tray. Similarly, hall sensors and magnetic beads are installed on the shell of the fertilizer dispenser and the outer groove wheel. These sensors detect the real-time position of the seed and fertilizer, allowing for the calculation of their relative positions in the soil.

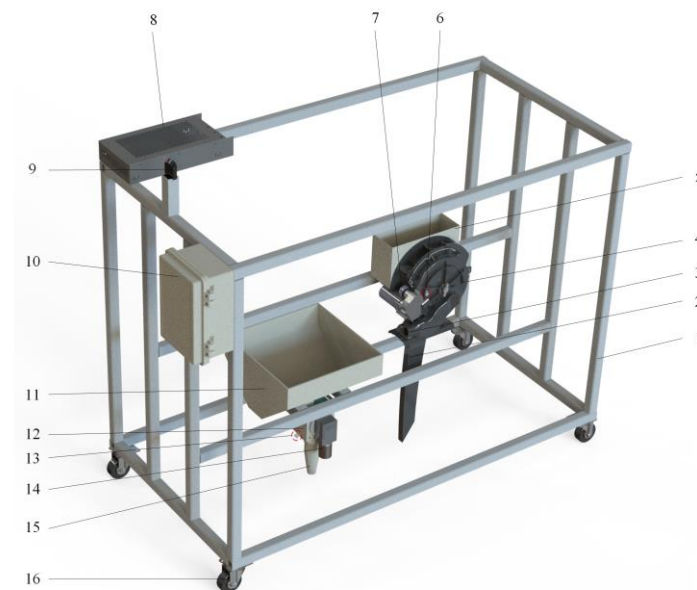


Figure 3. Structure diagram of seed fertilizer co-sowing device. 1. Aluminum profile machine. 2. Seed guide tube. 3. Aspirating pipe. 4. Seed metering device. 5. Seed box. 6. Seed sensor. 7. Seeding motor and its encoder and reducer. 8. Power supply. 9. Beidou/GPS antenna. 10. Distribution box. 11. Fluted roller fertilizer apparatus. 12. Fertilizer apparatus. 13. Fertilizer sensor. 14. Fertilizer motor and its encoder and reducer. 15. Fertilizer guide tube. 16. Wheels.

2.4. Control Model of Fertilizer Alignment

Taking the Dvor 2BQD-18 electric drive pneumatic precision seeder (Heilongjiang Dewo technology development Co., Ltd., Haerbin, China) [34] as an example, the operation process was to fertilize first and then seed. There was a certain installation distance between the fertilizer drop mouth and the seed guide mouth. To realize the correspondence between

seed and fertilizer, it is necessary to determine the relative position of seed and fertilizer according to the time of seed and fertilizer drop. We assumed that the speed of the seeder did not change abruptly, and there was no bounce after the seed and fertilizer entered the soil.

When the groove of the outer groove wheel fertilizer distributor rotates to the fertilizer outlet of the fertilizer guide plate, the sensor generates a signal and transmits it to the single-chip microcomputer, and the single-chip microcomputer starts timing. When the seeds on the turntable of the metering device rotate to the metering port, the sensor generates a signal and transmits it to the single-chip microcomputer. The single-chip microcomputer stops timing. The seed fertilizer alignment model is shown in Figure 4.

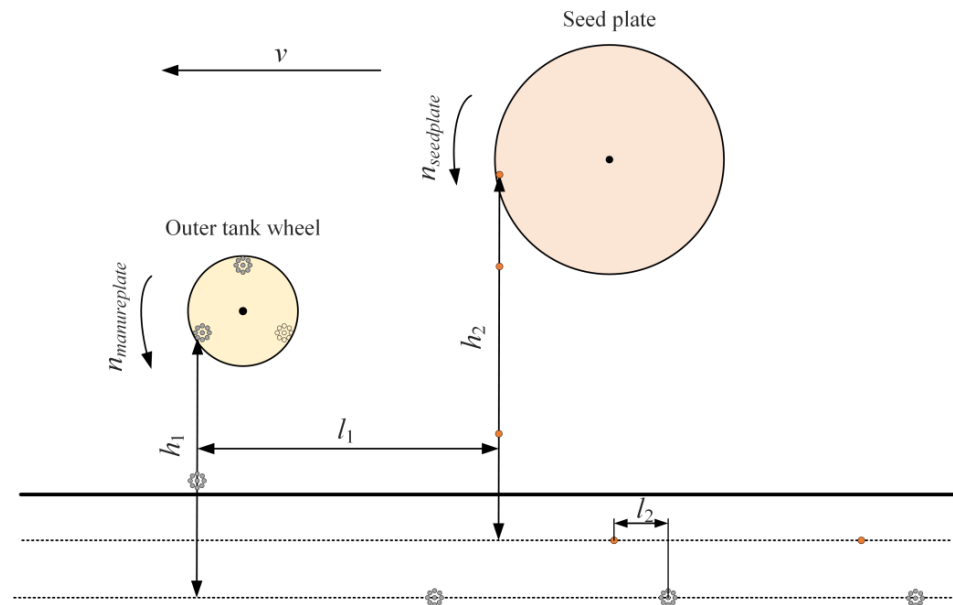


Figure 4. Seed fertilizer counterpoint model.

The fall of fertilizer is a free-fall movement. According to the fall time of fertilizer, the distance between the outer groove wheel fertilizer feeder and the suction seed dispenser, the fall time of seeds, and the operation speed of the machine, the time relationship that meets the relative position of the precise simultaneous sowing of seed and fertilizer was obtained as Equation (1).

$$vt_{theory} + vt_2 = v(t_1 + t_3) + l_1 + l_2 \tag{1}$$

where v is the machine speed; t_{theory} is the theory of planting waiting time; t_1 is the fertilizer time; t_2 is planting time; t_3 is the sum of sensor detection time, processor calculation time, and friction delay time of fertilizer falling between the shell and the fertilizer guide tube; l_1 is the longitudinal distance between seed and fertilizer; l_2 is the longitudinal distance between seeds and fertilizer. Assuming the fertilizer is in a free-fall motion, t_3 is obtained by the conventional method.

$$t_1 = \sqrt{\frac{2h_1}{g}} \tag{2}$$

$$t_2 = \sqrt{\left(\frac{v_y}{g}\right)^2 + \frac{2h_2}{g}} - \frac{v_y}{g} \tag{3}$$

$$t_{theory} = \left(\sqrt{\frac{2h_1}{g}} + t_3 + \frac{l_1 + l_2}{v} - \sqrt{\left(\frac{v_y}{g}\right)^2 + \frac{2h_2}{g}} + \frac{v_y}{g} \right) \tag{4}$$

In this equation, v_y is the initial velocity of the seed in the vertical direction, h_2 is the height of the seed from the seed groove, and g is the falling acceleration, usually $9.8 \text{ m}\cdot\text{s}^{-2}$. The actual speed of the planting plate can be calculated by the following Equation (5).

$$n_{seedplate} = \frac{60 \cdot 1000N_2}{M_2O_{c2}T_2i_2} \quad (5)$$

with N_2 for seeding motor encoder T_2 cycle captured pulse number; M_2 for a row of DC motor encoder resolution; O_{c2} for seeding motor encoder counting mode; T_2 for seeding DC motor speed sampling period, ms; i_2 for sowing gear transmission ratio. When seed and vertical direction are at the angle of θ , seeding disc radius is R , cm. The seed in the vertical direction of the initial speed v_y can be expressed as Equation (6).

$$v_y = \frac{60 \cdot 1000N_2\pi R \cos \theta}{3000M_2O_{c1}T_2i_2} \quad (6)$$

v_y is expressed in $\text{m}\cdot\text{s}^{-1}$. The difference between the theoretical waiting time and the actual waiting time is $\Delta t = t_{theory} - t_{current}$, where $t_{current}$ is the actual planting waiting time, s. Comparing the waiting time of the theoretical seed arrangement with the actual seed arrangement waiting time, when $\Delta t \neq 0$, there is a deviation in the position of the seed fertilizer, so the relative position of the seed fertilizer needs to be corrected.

2.5. Speed Control Model

After the system is started, the parameters such as seed spacing, working speed, and number of seed holes are set. The seed metering device of the fertilizer discharger enters the working state. The system obtains the real-time speed value detected by the satellite speed measurement module. The STM32 microcontroller calculates the target speed of the fertilizer discharge motor based on the working speed, and outputs a PWM signal to drive the DC motor. The outer slot wheel fertilizer discharger is then driven after the reducer decelerates. The encoder collects the actual speed of the fertilizer motor, and the PID control algorithm adjusts the output PWM control signal in real time based on the deviation. This ensures that the speed of the fertilizer motor can quickly and accurately follow the operating speed, and the speed of the seeding motor can be controlled in the same manner. The overall scheme of the seed and fertilizer sowing control system is illustrated in Figure 5, based on the structure of the seed and fertilizer precision sowing control system.

Note that v is the machine forward speed, $\text{m}\cdot\text{s}^{-1}$; i_1 is the transmission ratio of the fertilization reduction gear; i_2 is the transmission ratio of the sowing deceleration gear; X_r sets the particle spacing, cm; Z_1 is the number of external groove wheel grooves; Z_2 is the number of holes in the row plate; M_1 is the resolution of the fertilizer exhaust motor encoder; M_2 is the resolution of the row-type DC motor encoder; N_1 is the number of pulses captured in the encoder T_1 cycle; N_2 is the number of pulses captured in the encoder T_2 cycle; O_{c1} is the counting mode of the fertilizer exhaust motor encoder; O_{c2} is the counting mode of the row-type motor encoder; n_{manure} is the target rotation speed of the fertilizer exhaust motor, $\text{r}\cdot\text{min}^{-1}$; $n_{m-current}$ is the feedback speed of the fertilizer motor, $\text{r}\cdot\text{min}^{-1}$; n_{seed} is the target speed of the row motor, $\text{r}\cdot\text{min}^{-1}$; $n_{s-current}$ is the feedback speed of the type motor, $\text{r}\cdot\text{min}^{-1}$; $u_1(t)$ is the PWM control signal pulse of the fertilizer exhaust motor; $u_2(t)$ and $u_3(t)$ are the PWM control signal pulse of the motor; $e_1(t)$ is the deviation between the theoretical speed and the feedback speed of the fertilizer motor, $\text{r}\cdot\text{min}^{-1}$; $e_2(t)$ is the deviation between the theoretical speed and the feedback speed of the type motor, $\text{r}\cdot\text{min}^{-1}$; $e_3(t)$ is the deviation between the sorting target time interval of the sorting motor and the actual time interval, ms; $ec(t)$ is the rate of change of the deviation value of the row motor, ms^{-1} ; t_{theory} is the time difference of theoretical fertilizer discharge; h_1 is the difference between the height of the seed tube and the seed groove; h_2 is the height difference between the beginning of the fertilizer guide tube and the fertilizer ditch; l_1 is the longitudinal distance between the

seed tube and the fertilizer tube; l_2 is the longitudinal distance between seeds and fertilizer; $t_{current}$ is the time difference of the actual fertilizer discharge and planting.

The theoretical speed of the fertilization motor is n_{manure} ($r \cdot \min^{-1}$).

$$n_{manure} = \frac{60 \cdot 100v i_1}{X_r Z_1} \tag{7}$$

The actual speed is $n_{m-current}$ ($r \cdot \min^{-1}$).

$$n_{m-current} = \frac{60 \cdot 1000N_1}{M_1 O_{c1} T_1} \tag{8}$$

The theoretical speed of the seeding motor is n_{seed} ($r \cdot \min^{-1}$).

$$n_{seed} = \frac{60 \cdot 100v i_2}{X_r Z_2} \tag{9}$$

The actual speed of the seeding motor is $n_{s-current}$ ($r \cdot \min^{-1}$).

$$n_{s-current} = \frac{60 \cdot 1000N_2}{M_2 O_{c2} T_2} \tag{10}$$

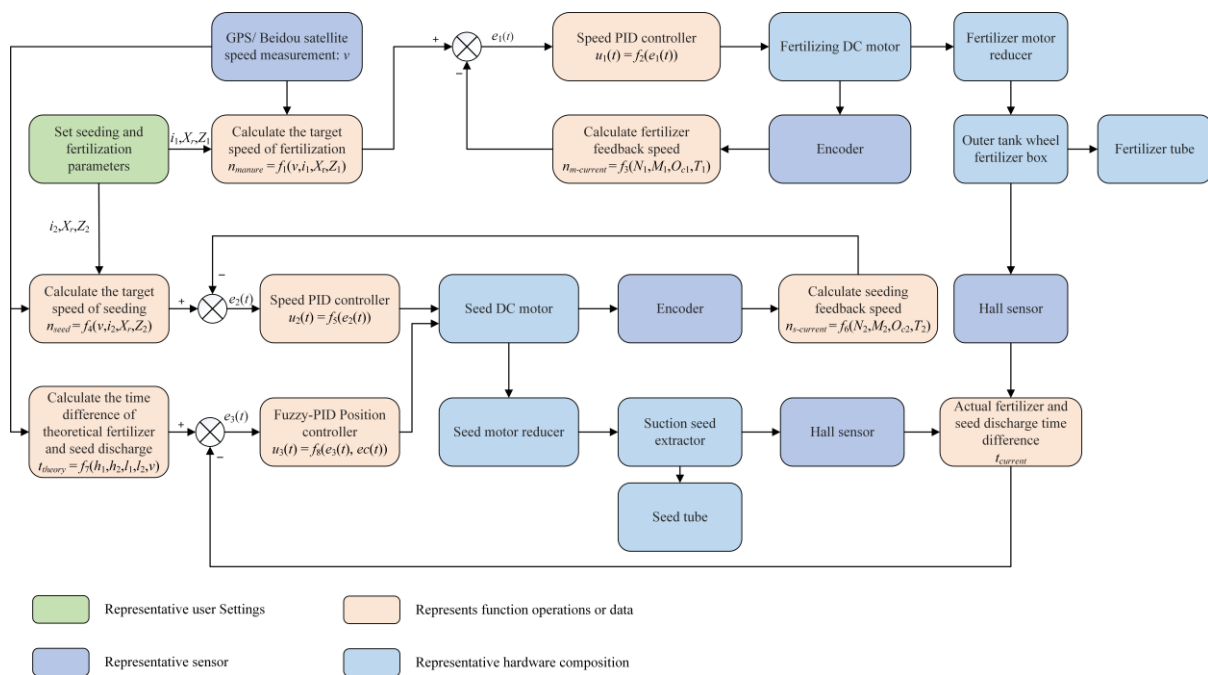


Figure 5. The overall scheme of fertilizer simultaneous sowing control system.

2.6. Control Algorithm

The speed control for sowing and fertilization utilizes the traditional PID algorithm, while the position control for seed and fertilizer utilizes the fuzzy PID control algorithm with gain adjustment. This approach addresses the limitations of the conventional PID parameters, which cannot be adjusted in real time. Additionally, the response time of the fuzzy PID controller is shorter compared to the conventional PID controller, making it more suitable for nonlinear systems. This allows for precise control of the seeding motor based on the position information of the seed and fertilizer under the rotation of the seed plate and the outer groove wheel, ensuring proper alignment of the seed and fertilizer. The controller structure is illustrated in Figure 6. The error e between the target value and the output value and the change rate de/dt of e is taken as the input of the fuzzy controller, and

the PID parameters are adjusted online using the fuzzy control rules. The fuzzy controller first fuzzifies the input, then performs fuzzy reasoning, and finally defuzzifies the results of the fuzzy reasoning to output the three parameters of the PID controller: K_p , K_i , and K_d . To achieve the effect of adaptive tuning of PID controller parameters, meet the different requirements of deviation e and deviation e change rate de/dt on PID parameters [33].

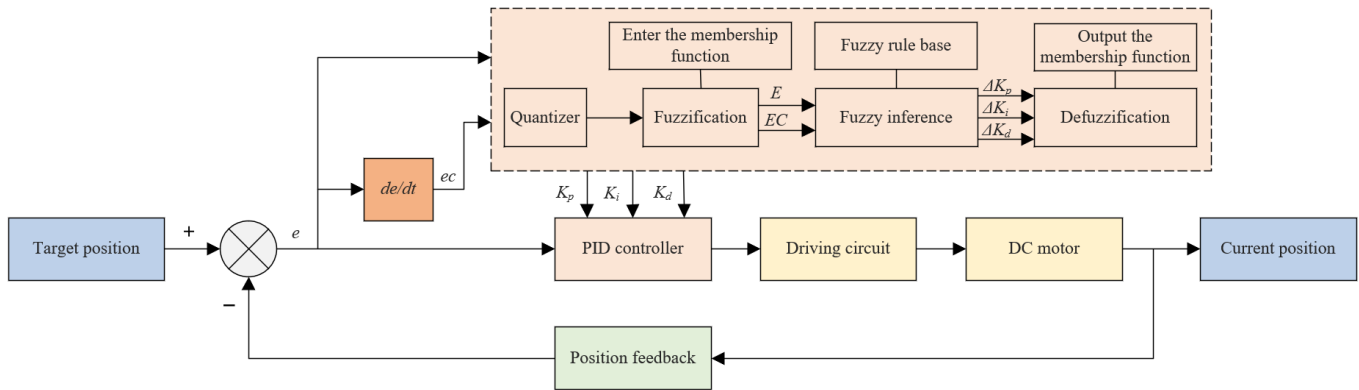


Figure 6. The structure of the fuzzy PID controller.

The fuzzy controller mainly comprises three modules: fuzzification, fuzzy inference, and defuzzification. The negative large [NB], negative medium [NM], negative small [NS], zero [ZO], positive small [PS], positive medium [PM], and positive large [PB] fuzzy subsets were selected. Considering the coverage and sensitivity of the universe, and to simplify the calculation of STM32F103ZET6, each fuzzy subset uses a triangular membership function [35,36]. According to the fuzzy rules of PID parameters, the corresponding output can be inferred according to the input deviation e and the deviation change rate, etc. Firstly, the membership degree of K_p , K_i , K_d corresponding to the fuzzy rules of j ($j = 1, 2, \dots, 49$) is obtained as Equation (11) [37].

$$\mu_{K_{p,i,d}(j)} = \min\{\mu_{r(j)}(E), \mu_{r(j)}(EC)\} \tag{11}$$

where $\mu_{r(j)}$ represents the value of membership degree adjusted according to fuzzy rules under different E and EC conditions. The input of the PID controller is an accurate variable, so it is necessary to defuzzify the output of the fuzzy controller. This study uses the center of gravity method [38,39]. At a certain sampling time, according to the membership degree of the deviation, ΔK_p , ΔK_i , ΔK_d can be obtained at this time.

$$\Delta K_{p,i,d} = \frac{\sum_{j=0}^n \{\mu_{K_{p,i,d}(j)} \cdot \Delta K_{p,i,d}(j)\}}{\sum_{j=0}^n \mu_{K_{p,i,d}(j)}} \tag{12}$$

Among them, ΔK_p , ΔK_i , ΔK_d are the membership degree of the output of the j -th fuzzy rule. The coefficients $\alpha_{p,i,d}$ can also be introduced to enlarge and reduce the variation in K_p , K_i , K_d . The specific implementation formula is as follows:

$$K_{p,i,d}(n) = K_{p,i,d}(n - 1) + \Delta K_{p,i,d} \cdot \alpha_{p,i,d} \tag{13}$$

The fertilizer sowing machine collects the working speed information through the sensor, determines the current speed deviation e and the change in the current deviation and the last deviation ec , and performs fuzzy reasoning according to the given fuzzy rules. Finally, the fuzzy parameters were defuzzified and the PID control parameters were output. The default parameter settings of the fuzzy PID algorithm are shown in Table 1.

Table 1. Default parameter settings of fuzzy PID algorithm.

Input/Output Variable	e	ec	K_p	K_i	K_d
Linguistic variable	E	EC	ΔK_p	ΔK_i	ΔK_d
The fundamental domain of discourse	$[-60, 60]$	$[-30, 30]$	$[-1, 1]$	$[-0.1, 0.1]$	$[-2, 2]$
Fuzzy subset	[NB NM NS ZE PS PM PB]				
Fuzzy domain	$[-6, 6]$	$[-3, 3]$	$[-3, 3]$	$[-0.3, 0.3]$	$[-6, 6]$
Quantization factor	0.1	0.1	3	3	3

2.7. Test Method

For the electric drive system, the speed control accuracy and response speed of the motor directly affect the performance of seeding and fertilization of crops. To determine the optimal PID control parameters, PID parameter tuning experiments using different input step signals were conducted; the overshoot (σ), rise time (t_r), adjustment time (t_s), and steady-state error (e_{ss}) of the system when input step signal was selected serve as the indexes to evaluate the speed regulation performance. The target speed of the fertilizer motor was set to $1500 \text{ r}\cdot\text{min}^{-1}$, the target speed of the seeding motor was set to $2000 \text{ r}\cdot\text{min}^{-1}$, and the speed sampling period was 20 ms. K_p , K_i , and K_d were determined according to the ‘first proportional, then integral, and then differential’ steps. The PID parameter adjustment of the position loop and the speed loop was determined by the mechanical transmission connection mode of the external load and the movement mode of the load, the load inertia, the requirements for speed and acceleration, and the rotor inertia and output inertia of the motor itself. The simple adjustment method was to adjust the gain parameter from small to large within the range of general experience according to the external load, and the integral time constant from large to small. The steady-state value without vibration overshoot was set as the optimal value [33].

It was difficult to observe and sample the fertilizer once it was covered in the soil. To accurately measure the spacing and distribution of seeds and fertilizers, they would fall on the surface. The fertilizer apparatus was in the front, the seed metering device was in the rear, the longitudinal distance between the two was adjusted to 30 cm, and the transverse distance was adjusted to 10 cm. The height of the fertilizer apparatus from the ground was adjusted to 25 cm, and the height of the fertilizer guide pipe mouth was adjusted to 5 cm from the ground. The height of the seed metering device from the ground was adjusted to 60 cm, and the height of the seed guide pipe was 5 cm from the ground.

A fertilizer mass distribution experiment and co-sowing accuracy experiment were conducted to investigate the impact of different seed spacing and working speeds on fertilization performance and co-sowing accuracy. The sampling time of the speed of the seeding motor and fertilizer motor was set to 20 ms, and the feedback period of the operation speed was set to 1.0 s. The negative pressure was set to 4.0 kPa, the horizontal distance between seeds and the center of fertilizer application in holes was set to 3 cm, and the fertilizer application amount in each hole was set to 5 g. At the same speed, the grain spacing was adjusted to 20, 25, and 30 cm successively, and the distribution of fertilizer on the ground was measured at $2 \text{ km}\cdot\text{h}^{-1}$, $3 \text{ km}\cdot\text{h}^{-1}$, and $4 \text{ km}\cdot\text{h}^{-1}$. In the direction of machine operation, the least dense area of fertilizer in the two holes was selected as the beginning and end of the single-hole fertilizer interval, and the fertilizer interval was successively divided into several sub-intervals at an interval of 2.5 cm. The number of fertilizer particles and the longitudinal distance between seeds and the fertilization center in each subinterval were measured in the stable operation area. The size of fertilizer particles was assumed to be evenly distributed in the fertilizer. The number of fertilizer particles in 10 holes conforming to the grain spacing standard was collected in each group. Five sections were randomly selected in each group, and 20 pairs of seed fertilizer longitudinal distances were recorded in each section. According to the industry technical specification document [40], the qualified index for hole fertilization was determined by measuring whether the distance between the seed and the fertilizer center fell within the range of $3 \pm 2 \text{ cm}$.

3. Result and Analysis

3.1. PID Control Parameter Tuning Test

The step response curve of PID algorithm parameter tuning is shown in Figures 7 and 8. Figure 7a shows that the steady-state error decreases with the increase in K_p . When the motor reaches a steady state, its speed value is always less than the target speed. A K_p that is too large will increase the overshoot and steady-state error of the system. When $K_{p1} = 5$, the steady-state characteristics were better. The integral link was added to eliminate the steady-state error. Figure 7b shows that the integral effect increases with the increase in K_{i1} . When $K_{p1} = 5$ and $K_{i1} = 0.4$, the system response was faster, and the overshoot was minor. To further speed up the adjustment speed and increase the differential link, it can be seen from Figure 7c that K_{d1} should not be too large under the target speed condition. When $K_{d1} = 0.1$, the dynamic characteristics of the rising stage were better, and the overshoot was more minor. Similarly, when the PID parameters of the seeding motor were $K_{p2} = 2.0$, $K_{i2} = 0.1$, and $K_{d2} = 0.05$, the system had better steady-state characteristics, faster response, minor overshoot, and better dynamic characteristics, which meets the requirements of precise simultaneous seeding of seed and fertilizer. The step response results are shown in Table 2.

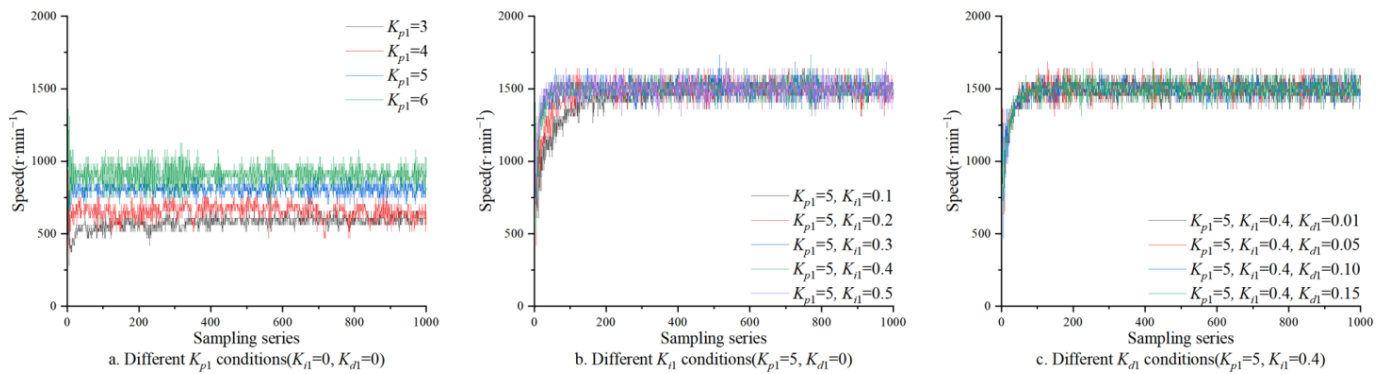


Figure 7. Fertilization PID parameter setting and step response test.

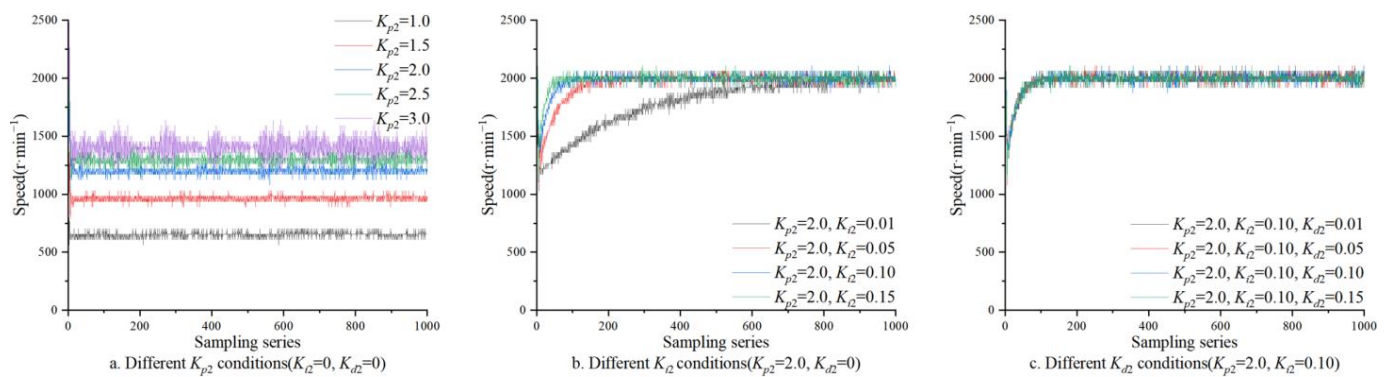


Figure 8. Seeding PID parameter tuning and step response test.

Table 2. PID algorithm parameter tuning step response results.

Index	PID Parameters of Fertilizer Motor		PID Parameters of Seeding Motor	
	$K_{p1} = 5, K_{i1} = 0.4, K_{d1} = 0.1$		$K_{p2} = 2.0, K_{i2} = 0.10, K_{d2} = 0.05$	
Rise time t_r/s	0.06		0.34	
Settling time t_s/s	1.16		1.66	
Overshoot $\sigma/\%$	5.60		9.5	
Steady-state error $e_{ss}/\%$	0.20		0.20	

After the speed loop was stabilized, the PID parameters of the system's seed fertilizer position loop were determined similarly. The adjustment range of the PID parameters of the seed fertilizer position loop was increased gradually. The response speed of the position loop should be slower than that of the speed loop. Otherwise, it could easily cause system oscillation; $K_{p3} = 0.2$, $K_{i3} = 0.01$, $K_{d3} = 0.01$.

3.2. Fertilizer Distribution Test

The test diagram of the device is shown in Figure 9 (the gas suction pipe has been pulled out). Figure 10 shows the fertilizer distribution when the operating speed was $3 \text{ km}\cdot\text{h}^{-1}$ and the seed spacing was set to 20 cm. As can be seen from Figures 10 and 11, the fertilizer was basically clumpy, and the fertilizer increased first and then decreased in the direction of operation. The fertilizer in scattered places may be the fertilizer discharged by the outer tank wheel driving layer. At the same seed spacing, fertilizer distribution had no significant difference with the increased operation speed. The average fertilization amount deviation of hole fertilization was 6.7%, and the coefficient of variation range was 3.16~6.09%. The variation coefficient of fertilization stability $\leq 7.8\%$ and the deviation of fertilization amount $\leq 15\%$ in the industry technical specification document [40] are satisfied. After analyzing the actual operational situation, to enhance fertilizer concentration, potential modifications include reducing the number of grooves on the outer groove wheel, increasing the ratio of the fertilizer area above the outer groove wheel to the fertilizer storage area, enlarging the diameter of the outer groove wheel, and minimizing the fertilizer rolling time within the fertilizer box and guide tube after discharge. The fertilizer opening under the fertilizer guide tube can be designed to facilitate the fertilizer concentration.



Figure 9. Pictures of machine operation.



Figure 10. The fertilizer distribution when the operating speed was $3 \text{ km}\cdot\text{h}^{-1}$ and the seed spacing was set to 20 cm.

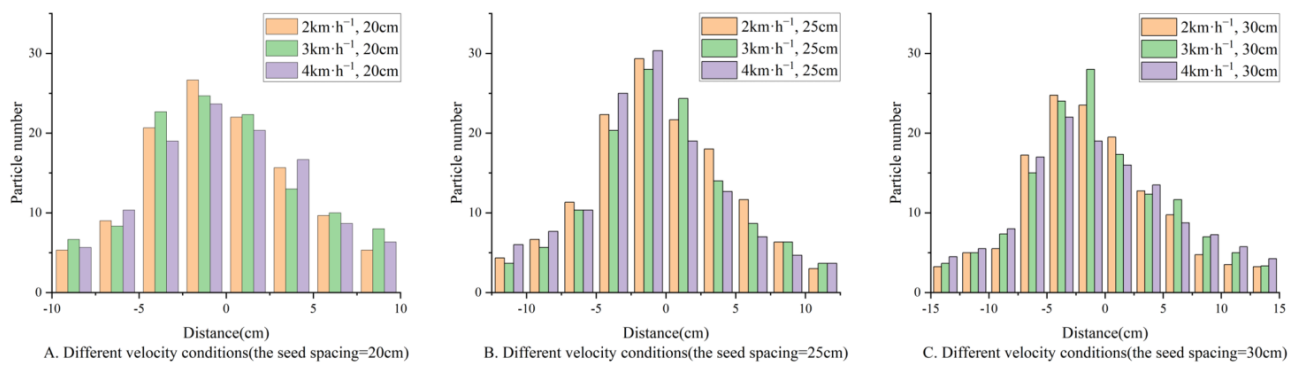


Figure 11. Fertilizer distribution under different seed spacing and different operating speeds.

3.3. Precision Test of Seed Fertilizer Co-Sowing

A test was conducted to evaluate the accuracy of co-sowing seeds and fertilizer at different seed spacing and operation speeds. The bench test and seed and fertilizer distribution are illustrated in Figure 12, and the precision test results are presented in Table 3. We have circled the fertilizer concentration area in Figure 12. The qualified index of hole fertilization decreased with an increase in operation speed while still meeting the required threshold of $\geq 80\%$. During operation, the fertilizer was mostly concentrated behind the seed, resulting in a good seed–fertilizer match and precise sowing of maize. To reduce the occurrence of seed bouncing during the test, the height of the seed discharging device can be appropriately reduced, and the length of the seed guide tube can be shortened. To better align the seed and fertilizer and determine the timing of seed and fertilizer discharge, we can first test them independently and then adjust the delay time t_3 for optimal results. However, the simplified experimental design also has some limitations. Due to the difference in environment, mechanical structure, and vibration of the device, the qualified rate of sowing fertilizer in the field may be lower than that in the soil tank test. In future studies, we will consider devices that contain multiple seeding and fertilization monomers and conduct a more comprehensive and detailed evaluation of their performance. The adaptability of the control system in complex field conditions and the accuracy of the seed fertilizer co-sowing can be further examined.

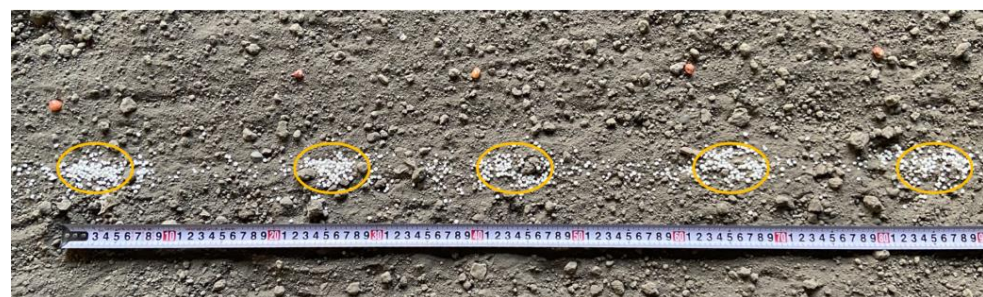


Figure 12. Bench test and distribution of seed fertilizer.

Table 3. Indexes of simultaneous sowing of three fertilizers.

Seed Spacing $v/(km \cdot h^{-1})$	Average Longitudinal Distance of Seed Fertilizer/mm			The Qualified Index of Hole Fertilization/%		
	20 cm	25 cm	30 cm	20 cm	25 cm	30 cm
2	35	34	34	90	91	89
3	34	35	36	91	91	89
4	35	36	36	88	90	87

4. Conclusions

In the present investigation, a precise simultaneous sowing control system for maize seed and fertilizer, based on a novel automatic alignment control algorithm, was designed, debugged, and experimentally verified. The main conclusions of this investigation can be addressed as follows.

(1) A precise simultaneous sowing control system for maize seed and fertilizer was built using STM32 as the core controller, encoder, hall sensor, and satellite positioning module as feedback components, and a DC motor as the actuator. A precise simultaneous sowing control algorithm for maize seed and fertilizer was designed. Through the PID parameter setting test, when the target speeds of the fertilizer and seeding motors were $1500 \text{ r}\cdot\text{min}^{-1}$ and $2000 \text{ r}\cdot\text{min}^{-1}$, the PID parameters of the fertilizer motor were $K_{p1} = 5$, $K_{i1} = 0.4$, $K_{d1} = 0.1$, the PID parameters of the seeding motor were $K_{p2} = 2.0$, $K_{i2} = 0.10$, $K_{d2} = 0.05$, and the initial parameters of the fuzzy PID position loop were $K_{p3} = 0.2$, $K_{i3} = 0.01$, $K_{d3} = 0.01$. The fertilizer distribution experiment obtained the fertilizer distribution under different grain spacing and working speeds, which met the requirements of precise fertilization.

(2) Based on the operating speed of the machine, the distance between the plant, the reduction ratio of the motor, the height of the seed metering device and fertilizer apparatus from the ground, and their relative positions, as well as the timing of seeding and fertilizing, a control model for precise simultaneous seeding and fertilizing was developed. Additionally, a control algorithm was proposed to accurately align the positions of the seed and fertilizer. The verification experiment showed that the machine's operating speed was $2 \text{ km}\cdot\text{h}^{-1}$, $3 \text{ km}\cdot\text{h}^{-1}$, and $4 \text{ km}\cdot\text{h}^{-1}$. The seed spacing was 20 cm, 25 cm, and 30 cm, and the qualified index of hole fertilization and the alignment of seed and fertilizer were better, which met the requirements of precise simultaneous sowing of seed and fertilizer.

(3) By conducting research on the control system for precise co-seeding operation of the maize electric drive seeder, relying on a variety of sensors to collect and build multi-source parameter models such as a vehicle speed signal and seed drop signal, the closed-loop joint control strategy of the seed discharge device and fertilizer discharge device was designed. The control theory of precise electric drive co-seeding operation of seed fertilizer was formed, realizing accurate alignment of seed fertilizer into the soil and making full use of the fertilizer effect. The efficiency and quality of seeding and fertilization were improved.

Author Contributions: Conceptualization, J.L., F.P. and C.J.; methodology, J.L. and J.C.; software, J.L.; validation, J.L., F.P. and H.Z.; formal analysis, J.L. and C.J.; investigation, J.L., F.P. and J.C.; resources, F.P. and C.J.; data curation, J.L. and F.P.; writing—original draft preparation, J.L.; writing—review and editing, J.L. and C.J.; visualization, J.L. and H.Z.; supervision, C.J.; project administration, F.P. and C.J.; funding acquisition, F.P. and C.J. All authors have read and agreed to the published version of the manuscript.

Funding: This research was funded by the Key Scientific and Technological Projects in Key Areas of the Xinjiang Production and Construction Corps (No. 2023AB038, 2020AB011), and the National Natural Science Foundation of China (NSFC) (No. 32101634), and the Young Science and Technology Top Talent Program of Tianshan Talent Training Program in Xinjiang Province, and the Xinjiang Academy of Agricultural and Reclamation Science Research Project (No. 2023YJ013).

Institutional Review Board Statement: Not applicable.

Data Availability Statement: Data are contained within the article.

Conflicts of Interest: The authors declare no conflicts of interest.

References

1. Shen, Z. Overview of Research and Development of Maize Fertilization Equipment. *Agric. Sci. Technol. Equip.* **2022**, *5*, 75–76. [[CrossRef](#)]
2. Yan, Y.; Shi, X.; Liu, H.; Dan, H.; Liu, X.; Zhang, J.; Liu, J.; Li, Y.; Yang, M. Application effect of one-time fertilization method on summer corn. *Jiangsu Agric. Sci.* **2022**, *50*, 109–114. [[CrossRef](#)]

3. Ren, X. Research on the fertilizer utilization rate of corn fertilizer planting and fertilizer. *Anhui Agric. Sci. Bull.* **2019**, *25*, 113–114. [[CrossRef](#)]
4. Liu, Z. Single-grain seed fertilizer co-sowing technology of summer maize. *KeXue ZhongYang* **2020**, *6*, 19–20. [[CrossRef](#)]
5. Xing, Y.; Zhao, J.; Miao, Z.; Li, G.; Han, H.; Xu, Y.; Wang, K. Analysis of co-sowing technology of deep seed fertilizer on the side of summer maize. *XianDai NongYe Keji* **2021**, *22*, 27–29. [[CrossRef](#)]
6. Wang, Y. *Effect of One-Time Layered Fertilization on Agronomic Characters, Nitrogen Absorption and Yield of Maize*; Henan Agricultural University: Zhengzhou, China, 2023. [[CrossRef](#)]
7. Yang, L. Scientific application and extension analysis of soil fertilizer. *Seed Sci. Technol.* **2023**, *41*, 112–114. [[CrossRef](#)]
8. Wang, Z. Effects of fertilization on main agronomic traits and yield of maize. *Yunnan Agric.* **2020**, *6*, 65–69.
9. Yu, C.; Zhi, S.; Xiao, L.; Li, Y.; Ouyang, Y.; Guo, M.; Xiong, B. Effects of different fertilization methods on main agronomic characters and yield of maize variety Xiangyu16. *Bull. Agric. Sci. Technol.* **2023**, *7*, 39–42.
10. Song, X. Effects of different fertilization techniques on maize yield and grain quality. *Farm Mach. Using Maint.* **2021**, *12*, 157–158.
11. Zheng, S.; Chen, H.; Zou, P. Technical regulations for simultaneous sowing of seed and slow and controlled release fertilizer for summer maize in north China plain. *Fertil. Health* **2022**, *49*, 31–34. [[CrossRef](#)]
12. Shi, W.; Zhang, Q.; Li, L.; Tan, J.; Xie, R.; Wang, Y. Hole fertilization in the root zone facilitates maize yield and nitrogen utilization by mitigating potential N loss and improving mineral N accumulation. *J. Integr. Agric.* **2023**, *22*, 1184–1198. [[CrossRef](#)]
13. Jin, F. Research on maize fertilization technology and fertilization machinery. *Seed Sci. Technol.* **2022**, *40*, 70–72. [[CrossRef](#)]
14. Iacomi, C.; Popescu, O. A New Concept for Seed Precision Planting. *Agric. Agric. Sci. Procedia* **2015**, *6*, 38–43. [[CrossRef](#)]
15. Li, G.; Cheng, Q.; Li, L.; Lu, D.; Lu, W. N, P and K use efficiency and maize yield responses to fertilization modes and densities. *J. Integr. Agric.* **2021**, *20*, 78–86. [[CrossRef](#)]
16. Adu-Gyamfi, R.; Agyin-Birikorang, S.; Tindjina, I.; Manu, Y.; Singh, U. Minimizing nutrient leaching from maize production systems in northern Ghana with one-time application of multi-nutrient fertilizer briquettes. *Sci. Total Environ.* **2019**, *694*, 133667. [[CrossRef](#)] [[PubMed](#)]
17. Lu, Z. Development, trade changes and future prospects of China's corn industry in the past 60 years. *J. Heilongjiang Grain* **2021**, *9*, 9–14.
18. Jing, W. Principle and development trend of electronic control fertilizing and seeding device. *Agric. Equip. Technol.* **2018**, *44*, 11–12.
19. Cujbescu, D.; Găgeanu, I.; Persu, C.; Matache, M.; Vlăduț, V.; Voicea, I.; Paraschiv, G.; Biriș, S.S.; Ungureanu, N.; Voicu, G.; et al. Simulation of sowing precision in laboratory conditions. *Appl. Sci.* **2021**, *11*, 6264. [[CrossRef](#)]
20. Yuan, Y.; Bai, H.; Fang, X.; Wang, D.; Zhou, L.; Niu, K. Research Progress on Maize Seeding and Its Measurement and Control Technology. *Trans. Chin. Soc. Agric. Mach.* **2018**, *49*, 1–18. [[CrossRef](#)]
21. Liu, Z.; He, J.; Wang, Q.; Zhen, K. Research status and prospect of maize hole fertilization device in China. *Jiangsu Agric. Sci.* **2019**, *47*, 5–8. [[CrossRef](#)]
22. Kamgar, S.; Noei-Khodabadi, F.; Shafaei, S.M. Design, development and field assessment of a controlled seed metering unit to be used in grain drills for direct seeding of wheat. *Inf. Process. Agric.* **2015**, *2*, 169–176. [[CrossRef](#)]
23. Karimi, H.; Navid, H.; Besharati, B.; Eskandari, I. Assessing an infrared-based seed drill monitoring system under field operating conditions. *Comput. Electron. Agric.* **2019**, *162*, 543–551. [[CrossRef](#)]
24. Luo, X.; Liao, J.; Zang, Y.; Qu, Y.; Wang, P. Developing from Mechanized to Smart Agricultural Production in China. *Strateg. Study CAE* **2022**, *24*, 46–54. [[CrossRef](#)]
25. Liu, Z.; Wang, X.; Li, S.; Huang, Y.; Yan, X.; Zhao, H. Design of Maize Automatic Hole Fertilization System Targeting at Seed Based on Planetary Gear Train. *Trans. Chin. Soc. Agric. Mach.* **2023**, *54*, 60–67. [[CrossRef](#)]
26. Wang, Z.; Zhang, B.; Liang, C.; Wang, H. Design and Experimental Study on Maize Variable Hole Fertilizer Control System. *J. Heilongjiang August First Land Reclam. Univ.* **2022**, *34*, 99–108. [[CrossRef](#)]
27. Wu, N.; Lin, J.; Li, B. Design and Test on No-tillage Planter Precise Hole Fertilization System. *Trans. Chin. Soc. Agric. Mach.* **2018**, *49*, 64–72. [[CrossRef](#)]
28. Dong, X.; Huang, F.; Liu, J.; Zhu, C.; Chen, C.; Yi, S. Design and Experiment of Rice Deep-Side Fertilization Device for Hole-Type Seedling and Fertilizer Application. *J. Southwest Univ. (Nat. Sci.)* **2023**, *45*, 58–73. [[CrossRef](#)]
29. Liao, Q.; Chen, Y.; Zhang, Q.; Wang, L.; Lin, J.; Du, W. Design and Experiment of Side Deep Hole Fertilization Device for Rapeseed. *Trans. Chin. Soc. Agric. Mach.* **2023**, *54*, 41–52.
30. Zhang, J.; Liu, H.; Gao, J.; Lin, Z.; Chen, Y. Simulation and Test of Corn Layer Alignment Position Hole Fertilization Seeder Based on SPH. *Trans. Chin. Soc. Agric. Mach.* **2018**, *49*, 66–72. [[CrossRef](#)]
31. Zhou, J.; Lu, H.; Gao, Z.; Hu, K.; Qian, J.; Wan, Y. Design of Self-propelled Small Corn Hole Fertilizer Applicator. *J. Henan Sci. Technol.* **2020**, *19*, 46–48.
32. Liang, Y.; Tang, Z.; Ji, C.; Zheng, X.; Liu, J.; Li, Q.; Zhang, L. Optimization and Experiment of Structural Parameters of Outer Groove Wheel Fertilizer Drainer. *J. Agric. Mech. Res.* **2023**, *45*, 7–14. [[CrossRef](#)]
33. Yao, Y.; Chen, X.; Ji, C.; Chen, J.; Zhang, H.; Pan, F. Design and experiments of the single driver for maize precision seeders based on fuzzy PID control. *Trans. Chin. Soc. Agric. Eng.* **2022**, *38*, 12–21. [[CrossRef](#)]
34. Liang, L.; Chen, Y.; Ren, W.; Li, Z.; Yu, Y.; Li, C.; Chi, C.; Yang, H. Development of 2BQD Series Electric Drive Intelligent High Speed Precision Seeder. *Farm Mach. Using Maint.* **2023**, *7*, 6–10. [[CrossRef](#)]

35. Manuel, N.L.; İnanç, N.; Lüy, M. Control and performance analyses of a DC motor using optimized PIDs and fuzzy logic controller. *Results Control. Optim.* **2023**, *13*, 100306. [[CrossRef](#)]
36. Zhang, R.; Gao, L. The Brushless DC motor control system Based on neural network fuzzy PID control of power electronics technology. *Optik* **2022**, *271*, 169879. [[CrossRef](#)]
37. Somwanshi, D.; Bundele, M.; Kumar, G.; Parashar, G. Comparison of Fuzzy-PID and PID Controller for Speed Control of DC Motor using LabVIEW. *Procedia Comput. Sci.* **2019**, *152*, 252–260. [[CrossRef](#)]
38. Wu, C.; Zhu, Y.; Gao, Q. Fuzzy Adaptive PID Control of Pneumatic Position Servo System Using High-speed On/Off Valves. *Chin. Hydraul. Pneum.* **2021**, *45*, 47–53.
39. Wang, Z.; Sun, Z. Variable Universe Fuzzy-PID Control of Facility Intelligent Drip Irrigation System. *Water Sav. Irrig.* **2020**, *7*, 81–84+88.
40. *NY/T 1003-2006*; Technical Specification for Quality Evaluation of Fertilization Machinery. Ministry of Agriculture and Rural Affairs of the People's Republic of China: Beijing, China, 2006.

Disclaimer/Publisher's Note: The statements, opinions and data contained in all publications are solely those of the individual author(s) and contributor(s) and not of MDPI and/or the editor(s). MDPI and/or the editor(s) disclaim responsibility for any injury to people or property resulting from any ideas, methods, instructions or products referred to in the content.